Submitted to the
International Europhysics Conference on High Energy Physics
Aachen, Germany, July 17 – 23, 2003

Abstract: 567 **HENP, HQCD, HP, HF**

Observation of the photoproduction of $D^{*\pm}(2010)$ mesons associated with a leading neutron

ZEUS Collaboration

15. June 2003

Abstract

The photoproduction of a D^* meson with a neutron tag has been measured with the ZEUS detector at HERA using an integrated luminosity of 80 pb^{-1}. The decay modes, $D^{*+} \rightarrow D^0(\rightarrow K^-\pi^+)\pi^+$ and the corresponding anti-particles, were used to reconstruct the D^* meson. The leading neutron, carrying a large fraction of the incident proton's energy ($x_L > 0.2$) was detected in the Forward Neutron Calorimeter (FNC), 105 m downstream of the interaction point. The cross section for the reaction $ep \rightarrow D^*nX$ has been measured as a function of x_L, transverse momentum of the D^* meson, $p_T(D^*)$, and the photon-proton centre-of-mass energy, W. The ratios between neutron tagged and inclusive cross sections have also been measured. The results are compared with theoretical predictions.

1 Introduction

Events tagged with a leading neutron have been studied in ep collisions at HERA [1–4]. The neutrons carry a large fraction of the incoming proton beam energy, $x_L > 0.2$, and are produced at very small scattering angels, $\theta_n < 0.8$ mrad, indicative of a peripheral process. Charm production, by contrast, is an important process for investigating parton dynamics because the charm-quark mass provides a hard scale necessary to ensure the applicability of perturbative Quantum Chromodynamics (pQCD).

This contribution describes the observation of $D^{*\pm}$ photoproduction associated with a leading neutron and the comparison of differential cross sections and ratios with inclusive $D^{*\pm}$ photoproduction. The results extend to charm production previous ZEUS studies of dijet and inclusive photoproduction, as well as deep inelastic scattering tagged with a leading neutron.

2 Description of the experiment

The integrated luminosity of 80.2 pb^{-1} used for this measurement was collected at the ep collider HERA with the ZEUS detector during 1998 - 2000, when HERA collided 27.5 GeV positrons with 920 GeV protons, giving a center of mass energy of 318 GeV.

The forward neutron calorimeter (FNC) [5–7] was installed in the HERA tunnel at $\theta = 0$ degrees and at $Z = 106$ m from the interaction point in the proton-beam direction. Magnet apertures limit the FNC acceptance to neutrons with production angles less than 0.8 mrad, that is to transverse momenta $p_T \leq E_n\theta_{\text{max}} = 0.74x_L$ GeV.

3 Kinematics and event selection

The kinematics of photoproduction at HERA are specified by the photon-proton center of mass energy, W, which is related to the electron-proton center of mass energy, $\sqrt{s}$, by $W^2 = ys$ where y is the inelasticity, $y = (E - E')/E$ and $E(E')$ is the energy of the incoming (scattered) electron.

For the process $ep \to eD^{*\pm}nX$ four additional variables are chosen to describe the event, two for the produced neutron and two for the produced charmed meson. They are:

- (E_n,θ_n), the energy and production angle of the produced neutron; the energy is given in terms of $x_L = E_n/E_p$ where E_p is the energy of the incoming proton beam; only about 50% of the data have a θ_n measurement, therefore all results discussed here are integrated over this variable up to the maximum angle of neutron acceptance, 0.8 mrad;

- (p_T,η), the transverse momentum and pseudorapidity of the produced $D^{*\pm}$ meson.

Photoproduction events were selected using cuts based on the reconstructed vertex position of the interaction point, calorimeter energy deposits and the reconstructed tracks of charged particles. Calorimeter energy deposits and tracks were combined to form energy flow objects (EFOs). Events with a well-identified electron candidate in the uranium calorimeter were removed.

Events with a leading neutron were selected by requiring a large energy deposit ($x_L > 0.2$) in the FNC. The events with an energy deposition consistent with a proton, photon or neutrons that started showering in front of the FNC were removed [3].

4 $D^{*\pm}(2010)$ selection

The initial event sample was selected by identifying events containing a charmed meson.

The $D^{*\pm}$ selection cuts were applied based on the decay channel: $D^{*+} \rightarrow (D^0 \rightarrow K^-\pi^+)\pi_s^+$ (+ charge conjugate), where π_s indicates the "slow" pion [8]. The combinatorial background was reduced and the kinematic phase space defined by requiring:

- the transverse momentum of the $D^{*\pm}$ be greater that 1.9 GeV;
- the pseudorapidity of the $D^{*\pm}$ satisfy $|\eta(D^{*\pm})| < 1.5$;
- the transverse momentum of the kaon candidate satisfy $p_T(K) > 0.45$ GeV;
- the transverse momenta of the pion candidates satisfy $p_T(\pi_s) > 0.12$ GeV and $p_T(\pi) > 0.45$ GeV.

Since no particle identification was performed, the K and π masses were alternately attributed to the decay products of the candidate D^0 meson. Only D^0 candidates that had an invariant mass between 1.80 and 1.92 GeV were subject to the mass difference requirement $0.1435 < \Delta M < 0.1475$ GeV ($\Delta M = M(K\pi\pi_s) - M(K\pi)$).

The ΔM distribution for the neutron tagged sample is shown in Fig. 1. The data show right-signed track combinations; the histogram, wrong-signed combinations normalized to the right-signed combinations for $0.5 < \Delta M < 0.165$ GeV above the $D^{*\pm}$ mass window.

5 Monte Carlo simulation

A GEANT-based [9] Monte Carlo (MC) simulation was used to calculate selection efficiencies and correction factors for the charmed meson. Two different event generators were used: RAPGAP 2.08/06 [10] for evaluating the nominal corrections, and HERWIG 6.301 [11] as a systematic check. RAPGAP uses the Lund string model [12] for hadronization whereas HERWIG uses a cluster model. The events generated with RAPGAP were produced with an optional one-pion-exchange implementation for the leading neutron production. For all the MC samples, events with at least one $D^{*\pm}$ decaying in the appropriate decay channel were selected and passed through the standard ZEUS detector and trigger simulations as well as the event reconstruction package.

The selection efficiencies and correction factors for the neutron were calculated independently using methods developed previously [2, 3].

6 Systematic uncertainties

For the neutron measurement the major sources of systematic uncertainties are:

- uncertainty in the angular distribution of the neutrons. The uncertainty in the acceptance is $\pm 4\%$ except for the highest $x_L > 0.82$ bin where it grows to $\pm 7\%$;
- uncertainty in the overall energy scale of $\pm 2\%$ which results in an uncertainty in shape (a dilation) of the x_L spectrum. For the fixed bin $x_L > 0.2$ the the count uncertainty is $< 1\%$, but for $x_L > 0.82$ it is $\pm 15\%$;
- a normalization uncertainty because of proton beam gas interactions overlapping with a photoproduction event, proton beam associated noise, uncertainty in the amount of absorbing material in the beam line. The overall normalization uncertainty is $\pm 5\%$.

For the $D^{*\pm}$ measurement the major sources of systematic uncertainties and their effect on the integrated cross section are:

- the selection of photoproduction events. The W_{JB} and vertex cuts were varied, $\pm^{6}_{5}\%$;
- selection of the $D^{*\pm}$ candidates. The p_T thresholds of the tracked candidates were raised and lowered, $\pm 2\%$;
- the ΔM window used for the extraction of the $D^{*\pm}$ was widened, $+2\%$;
- the Monte Carlo model dependence. HERWIG was used instead of RAPGAP, -0.5%.

7 Results

Figure 2 shows the differential cross section for the reaction $ep \to eD^{*\pm}nX$ as a function of W, $p_T(D^*)$ and $\eta(D^*)$ in the kinematic region $Q^2 < 1$ GeV^2, $117.3 < W < 274.3$ GeV, $|\eta| < 1.5$, $p_T > 1.9$ GeV, $x_L > 0.2$ and $\theta_n < 0.8$ mrad. The experimental results are compared with the predictions of the Monte Carlo models RAPGAP and HERWIG. The agreement is satisfactory; however, as shown in Fig. 3 only RAPGAP with pion exchange explains the x_L distribution of the leading neutrons. This observation is agreement with the photoproduction of neutron tagged dijets [2].

Figure 4 shows the ratio of neutron tagged $D^{*\pm}$ production to inclusive $D^{*\pm}$ production as a function of the kinematic variables. Over the whole kinematic range the ratio is

$$r^{D^*}(x_L > 0.2) = 8.2 \pm 0.9(\text{stat}) \pm 0.3(\text{sys})\ \%$$

Within experimental error neutron tagged $D^{*\pm}$ production is compatible with being a constant fraction of inclusive $D^{*\pm}$ production.

8 Summary

The photoproduction of $D^{*\pm}$ mesons associated with a leading neutron has been observed with the ZEUS experiment in ep interactions at HERA in the kinematic region $Q^2 < 1$ GeV^2, $117.3 < W < 274.3$ GeV, $|\eta(D^*)| < 1.5$, $p_T(D^*) > 1.9$ GeV, $\theta_n < 0.8$ mrad, and $x_L > 0.2$; the Monte Carlo models RAPGAP, and HERWIG give a satisfactory description of the $D^{*\pm}$, but only RAPGAP with one pion exchange satisfactorily describes the energy of leading neutron. The ratio of neutron tagged $D^{*\pm}$ photoproduction to inclusive $D^{*\pm}$ photoproduction is $r^{D^*} = 8.2 \pm 0.9(\text{stat}) \pm 0.3(\text{sys})\%$, a significant fraction of the inclusive $D^{*\pm}$ cross section. This fraction is similar to that in DIS, but higher than that in PHP.

The ratio of neutron tagged $D^{*\pm}$ photoproduction to inclusive $D^{*\pm}$ photoproduction is compatible with being constant as a function of the kinematic variables.

Acknowledgments

We thank the DESY Directorate for their strong support and encouragement, and the HERA machine group for their diligent efforts. We are grateful for the support of the DESY computing and network services. The design, construction and installation of the ZEUS detector have been made possible owing to the ingenuity and effort of many people from DESY and home institutes who are not listed as authors.

References

[1] ZEUS Coll., M. Derrick et al., Phys. Lett. **B 384**, 388 (1995).

[2] ZEUS Coll., J. Breitweg et al., Nucl. Phys. **B 596**, 3 (2000).

[3] ZEUS Coll., J. Breitweg et al., Nucl. Phys. **B 637**, 3 (2002).

[4] H1 Coll., C. Adloff et al., Eur. Phys. J **C 6**, 587 (1999)..

[5] ZEUS FNC group, S. Bhadra et al., Nucl. Inst. Meth. **A 354**, 479 (1995).

[6] ZEUS FNC group, S. Bhadra et al., Nucl. Inst. Meth. **A 394**, 121 (1997).

[7] ZEUS FNC Group, S. Bhadra et al., *Proc. of the Seventh International Conference on calorimetry in High Energy Physics, Tuscon, Arizona, November 1997*, E. Cheu et al. (ed.), p. 295. World Scientific, Singapore (1998).

[8] S. Nussinov, Phys. Rev. Lett. **35**, 1672 (1975).

[9] R. Brun et al., GEANT3, Technical Report CERN-DD/EE/84-1, CERN, 1987.

[10] H. Jung, Comp. Phys. Comm. **86**, 147 (1995).

[11] G. Marchesini et al., Comp. Phys. Comm. **67**, 465 (1992).

[12] T. Sjöstrand, Comp. Phys. Comm. **39**, 347 (1986).

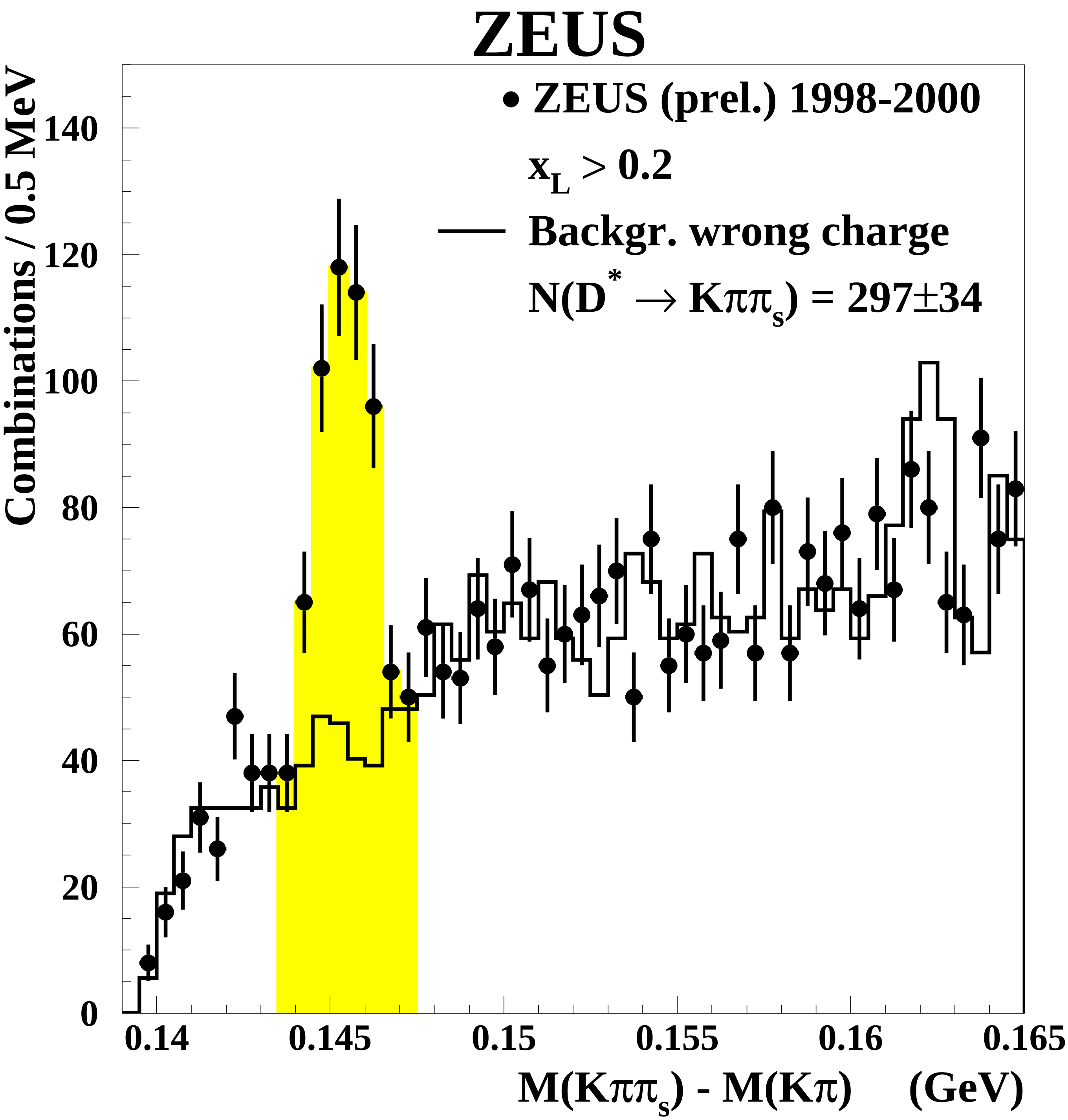

Figure 1: *The data points shows the neutron tagged ΔM distribution for right-signed track combinations. The histogram shows the wrong-signed combinations normalized to the right-signed combinations in the region $0.5 < \Delta M < 0.165$ GeV outside the $D^{*\pm}$ mass window $0.1435 < \Delta M < 0.1475$ GeV which is shown shaded.*

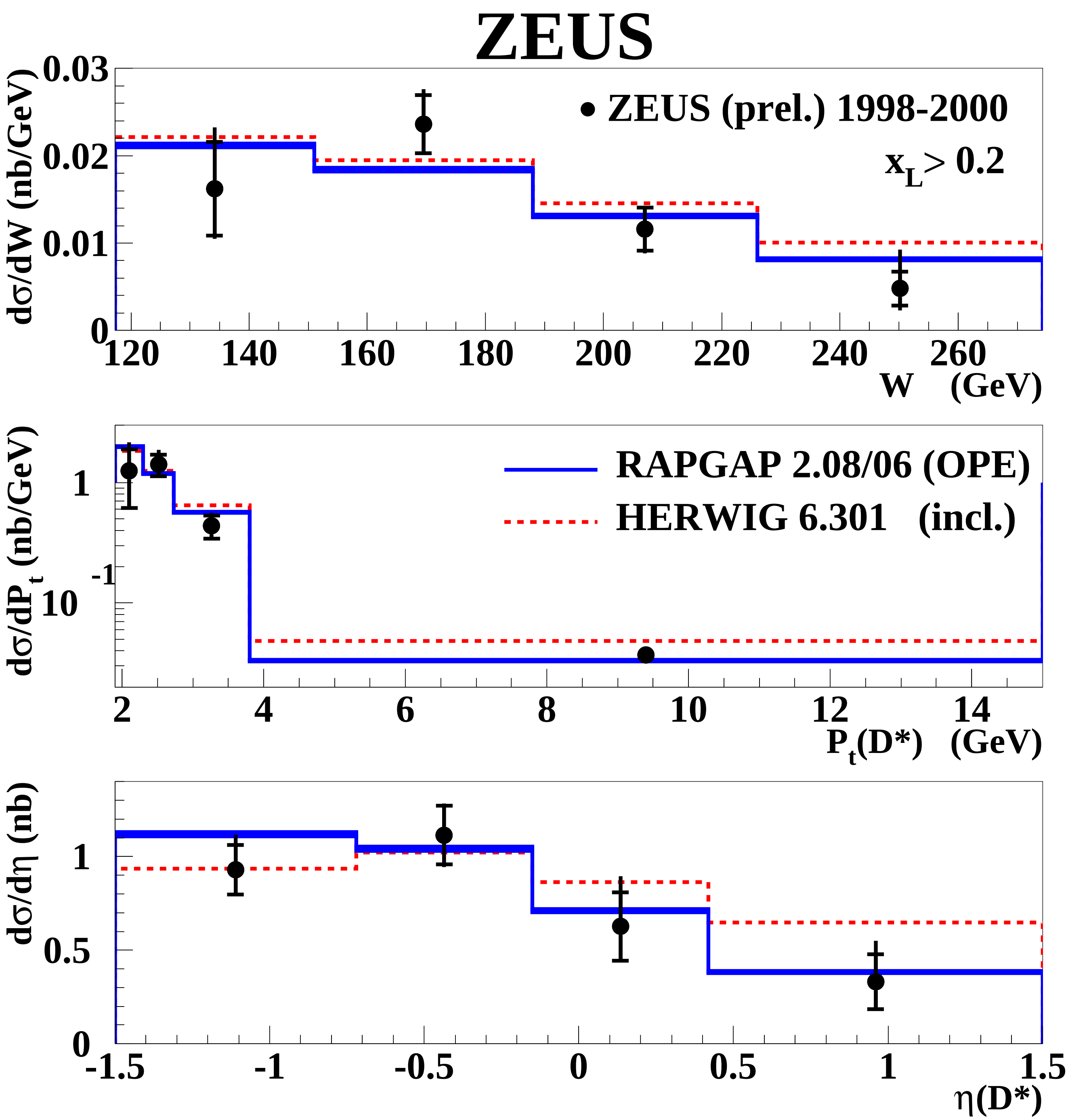

Figure 2: *The data points show the differential cross sections for neutron tagged $D^{*\pm}$ production as a function of W, $p_T(D^*)$ and $\eta(D^*)$ for $x_L > 0.2$ and $\theta_n < 0.8$ mrad. The predictions of Monte Carlo models RAPGAP with one pion exchange (solid histogram) and HERWIG (dashed histogram) are superposed for comparison.*

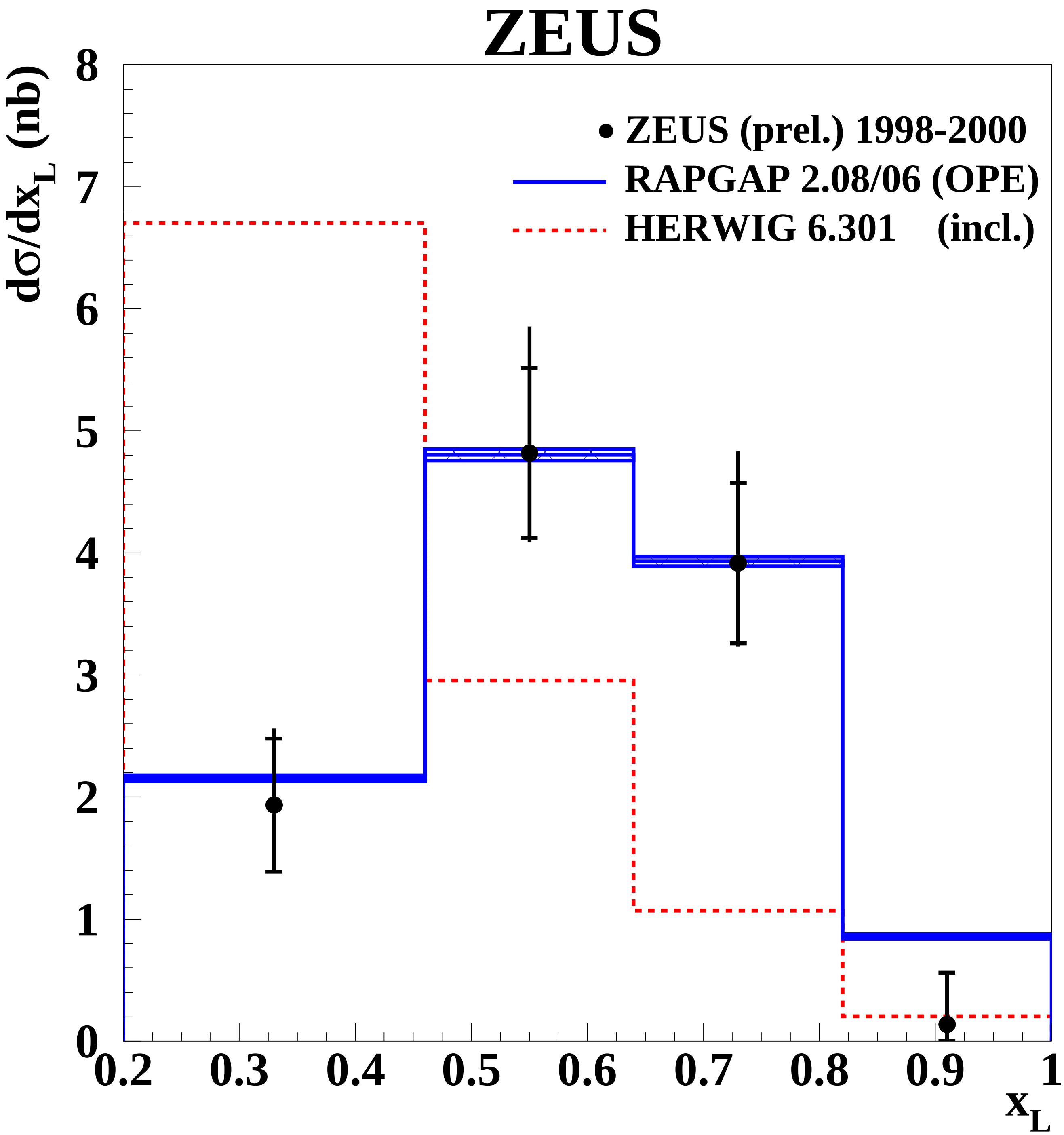

Figure 3: *The data points show the differential cross section for neutron tagged $D^{*\pm}$ production as a function of x_L for $117.3 < W < 274.3$ GeV, $|\eta(D^*)| < 1.5$, $p_T(D^*) > 1.9$ GeV, and $\theta_n < 0.8$ mrad. The predictions of the Monte Carlo models RAPGAP with one-pion exchange (solid histogram) and HERWIG (dashed histogram) are superposed for comparison.*

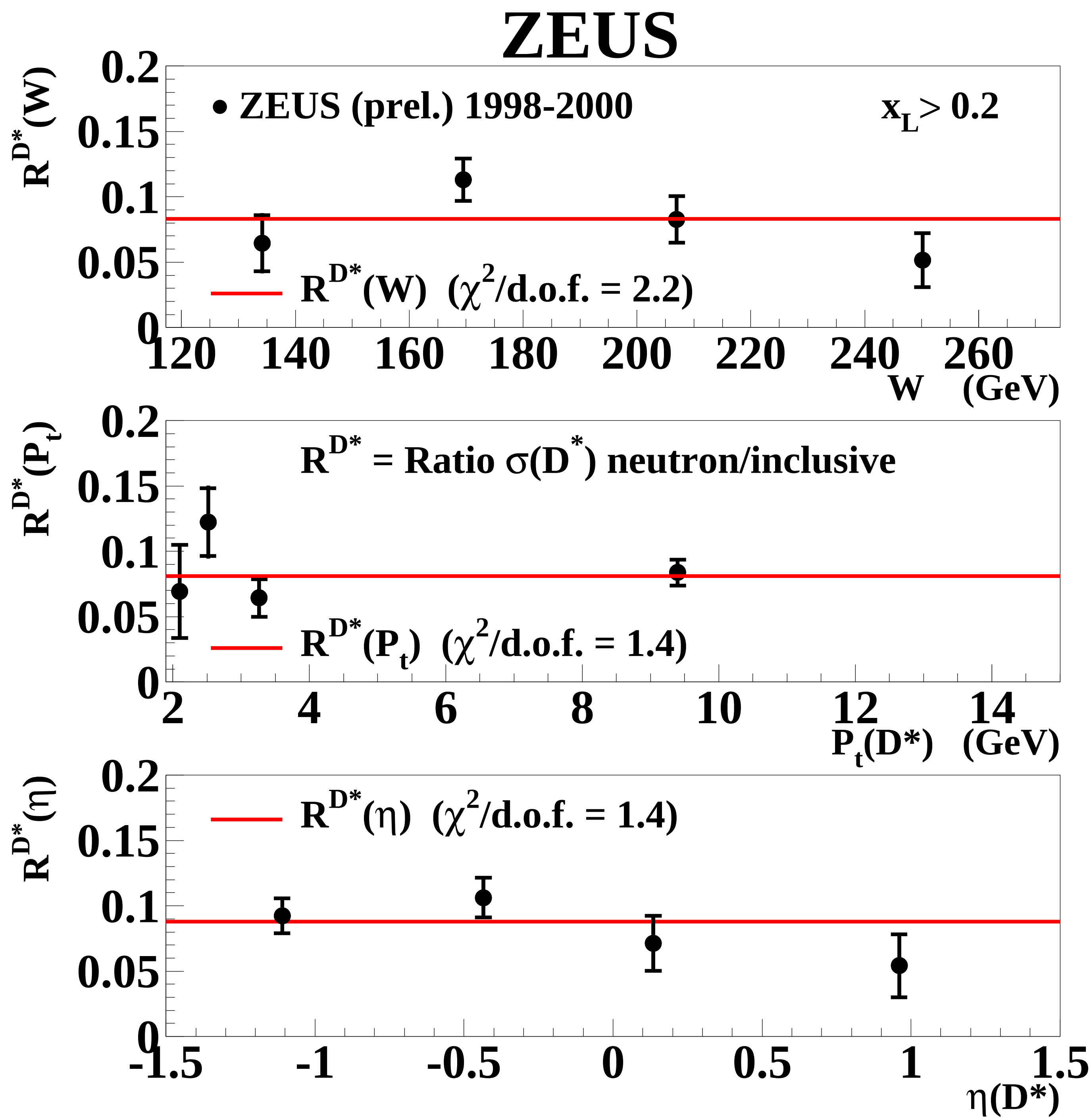

Figure 4: *The ratio of neutron tagged $D^{*\pm}$ production to inclusive $D^{*\pm}$ production as a function of W, $p_T(D^*)$ and eta(D^*) for $x_L > 0.2$ and $\theta_n < 0.8$ mrad. The line superposed on the figures shows the overall ratio of neutron tagged $D^{*\pm}$ to inclusive $D^{*\pm}$ events.*